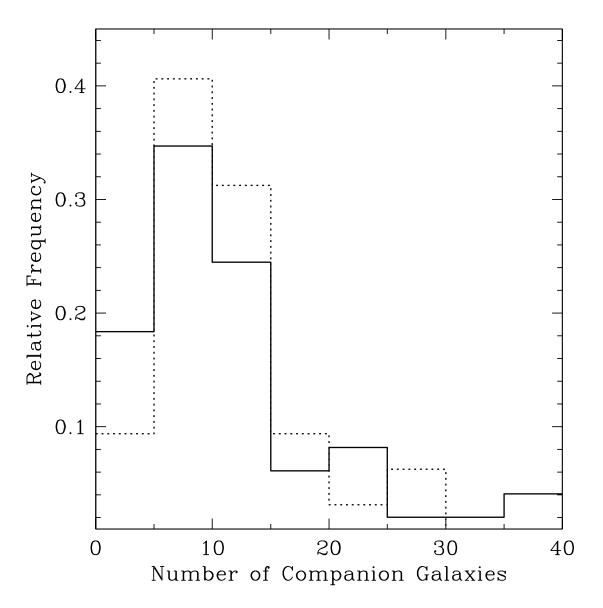
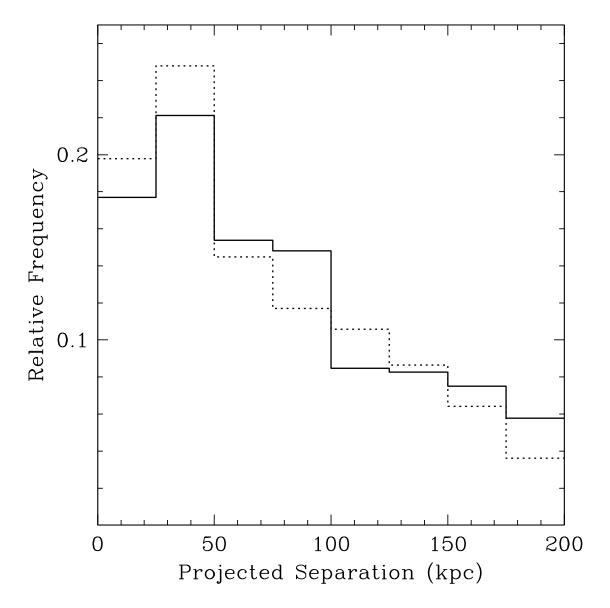
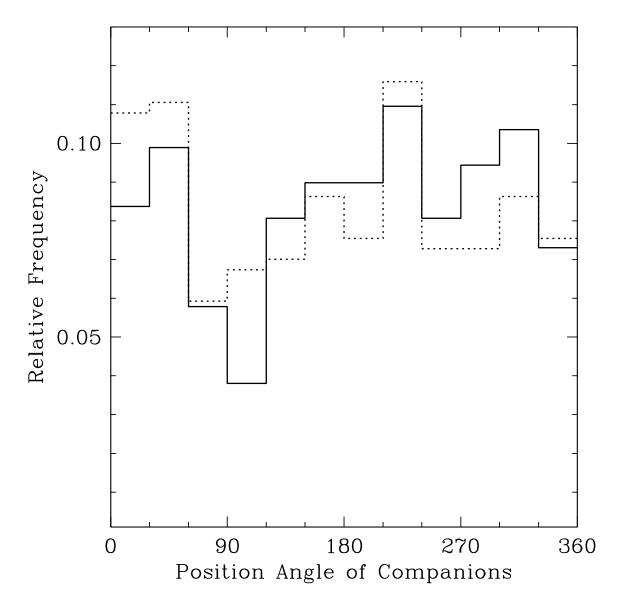


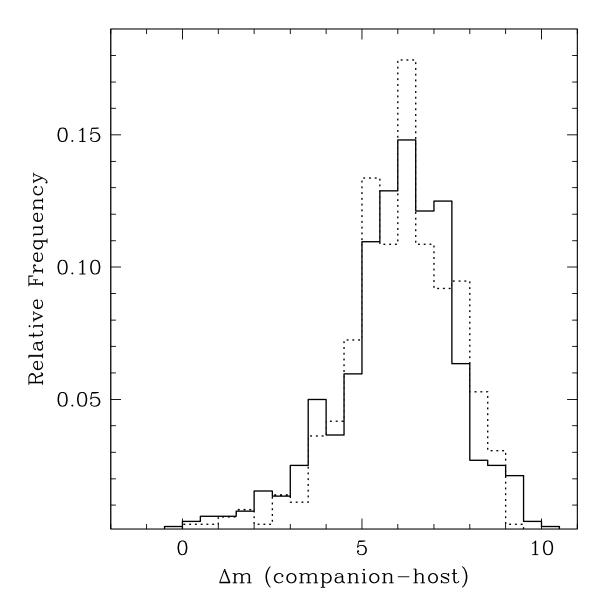
-22 -20 -18 -16 -14-12Absolute R Magnitude of Companions

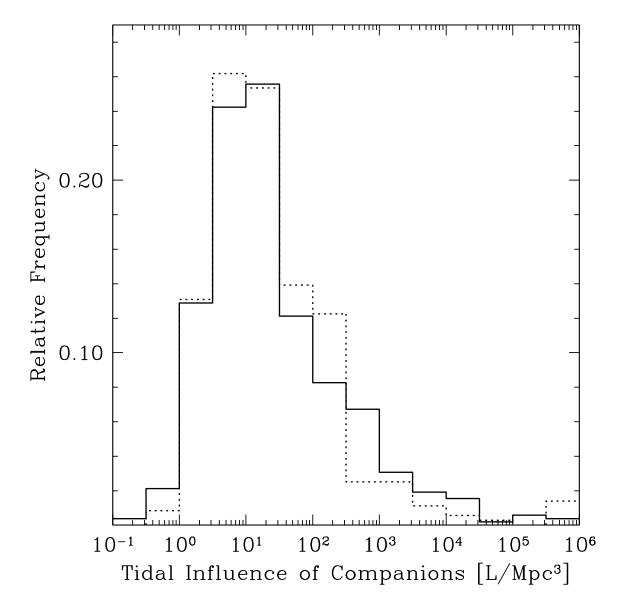
0.01











# A CCD Study of the Environment of Seyfert Galaxies:

# III. Host Galaxies and the Nearby Environments

S.N. Virani<sup>1</sup> and M.M. De Robertis

Dept. of Physics and Astronomy, York University

4700 Keele St., Toronto, ON, M3J 1P3, Canada

M.L. VanDalfsen

Dept. of Physics and Astronomy, McMaster University 1280 Main St. W., Hamilton, ON, L8S 4M1, Canada

<sup>&</sup>lt;sup>1</sup>Currently at Harvard-Smithsonian Center for Astrophysics, 60 Garden Street, MS 70 Cambridge, MA 02138

**ABSTRACT** 

A technique is described that permits the robust decomposition of the bulge

and disk components of a sample of Seyfert galaxies, as well as a (control) sample

of non-active galaxies matched to the Seyferts in the distributions of redshift,

luminosity and morphological classification. The structural parameters of the

host galaxies in both samples are measured. No statistically significant differences

at greater than the 95% level are found in these parameters according to a K-S

test.

"Companion galaxies" — defined as any galaxy within a projected separation

of 200 h<sup>-1</sup> kpc from the center of the host — are identified and their basic

properties measured. A comparison between the active and control samples in

the distributions of apparent R magnitude, absolute R magnitude (assuming the

"companions" are at the distance of the host), projected separation from the host,

position angle relative to the host, magnitude difference between the companion

and host, and strength of the tidal parameter, show no statistically significant

differences.

Similarly, no statistically significant differences are found between the control

and active sample host galaxies in terms of light asymmetries — bars, rings,

isophotal twisting, etc. The implications for a model in which interactions and

mergers are responsible for inciting activity in galactic nuclei are discussed briefly.

Accepted by the Astronomical Journal: 28 June 2000

Subject headings: galaxies: active – galaxies: evolution – galaxies: interactions

- galaxies: Seyfert

2

#### 1. INTRODUCTION

In order to understand the nature of activity in galactic nuclei, in particular how it is initiated and maintained, it is reasonable to begin with the question, how do active galaxies compare with non-active galaxies? But any such statistical comparison is fraught with difficulty since this, at least ideally, requires an understanding of the biases in the samples selected. Moreover, it is not clear just which parameter(s) should be compared. Could an active nucleus, especially in the more luminous members of the active galactic nuclei (AGN) family, have a significant effect on "macroscopic" scales; that is, not only on the immediate circumnuclear environment, but even on the structural parameters of the host galaxy?

For these reasons, a comparison of the environments of AGN has been of particular interest in the past two decades, motivated largely by the widely held hypothesis that interactions and mergers play a significant role in initiating activity in a nucleus.

Dultzin-Hacyan et al. (1999), De Robertis, Hayhoe & Yee (1998a) (hereafter Paper I), and Laurikainen et al. (1994) have observed that early qualitative efforts to study the environments of AGNs were plagued by sample biases and selection effects, especially in the selection of a "control" sample, i.e., a sample of non-active galaxies.

Seyfert galaxies have traditionally been the focus of such investigations for the reasons articulated in Paper I: they are sufficiently nearby that they can be studied in reasonable detail, and have a sufficiently high space density to permit the compiling of reasonably large samples. This is not to say that the environments of both intrinsically higher luminosity AGN such as QSOs, as well as lower luminosity systems such as LINERs and "dwarf Seyfert galaxies" have not been investigated. They have been, but not nearly in such detail.

Recent studies of Seyfert galaxies which have taken more care, particularly with the control sample such as Laurikainen & Salo (1995), De Robertis, Yee and Hayhoe (1998b) (hereafter, Paper II), and Dultzin-Hacyan et al. (1999) have achieved somewhat of a consensus compared with earlier studies: Seyfert galaxies in general do not inhabit significantly richer environments on scales ≥ 100 kpc than do non-active galaxies. Furthermore, it appears that Seyfert 2 galaxies have an excess of companions, while Seyfert 1 galaxies inhabit environments which are somewhat deficient in companions.

On smaller scales and from a dynamical perspective, observations by Keel (1996) and Kelm et al. (1998) indicate that there are no statistically significant differences between groups and pairs of galaxies in which a Seyfert is present, and those without an AGN. (Interestingly, Kelm et al. find that Seyferts tend to avoid groups and close pairs with a low velocity dispersion, as well as the closest pairs.)

Finally, on the smallest "macroscopic" scales, i.e., on scales of the host galaxies themselves, it is not clear whether there are significant structural differences in galaxies hosting a Seyfert nucleus and corresponding non-active galaxies. Recent work by McLeod & Rieke (1995), Mulchaey & Regan (1997), Mulchaey, Regan & Kundu (1997), and Hunt & Malkan (1999) among others, have shown that Seyfert nuclei are not located preferentially in kiloparsec-scale barred systems, though Hunt & Malkan (1999) do suggest Seyferts may be associated with rings more often.

In Papers I and II, we explored the question raised at the outset by quantitatively measuring the environments of both Seyferts and control galaxies within a projected separation of  $\approx 50-250$  kpc of the active nucleus by computing the galaxy-galaxy covariance function amplitudes. In this work, we consider two other comparisons between the active/non-active control samples: the characteristics of the "companion galaxies" within a projected distance of  $200 \, h^{-1}$  kpc (where  $H_0 = 50 \, \text{km s}^{-1} \, \text{Mpc}^{-1}$ ,  $q_0 = 0.5$  and  $h \equiv H_0/50 \, \text{km s}^{-1} \, \text{Mpc}^{-1}$ , hereafter) — including faint companions projected on the host itself and light asymmetries within the host — as well as the structural parameters of the

host galaxies.

In §2 we describe the observations and techniques used to analyse the data, while §3 presents the results. The summary and conclusions are contained in §4.

#### 2. OBSERVATIONS

A study of this kind must necessarily be statistical in nature since the redshift, and hence distance, of galaxies within a given angular radius is unknown in general. Foreground and background galaxy surface densities do vary with position on the sky, but such differences should average out given a sufficient number of fields distributed randomly on the sky, allowing intrinsic differences in the distribution of actual or "true" companion galaxies to become apparent.

A detailed description of the selection criteria for the active and control samples is provided in Paper I. Briefly, 32 Seyfert and 45 non-active galaxies were culled from the CfA survey.<sup>2</sup> The distributions of redshift, morphological classification, as well as luminosity of the non-active sample were chosen to match the Seyfert sample. (Because a small, but non-negligible fraction of light in Seyfert galaxies comes from the nucleus, the luminosity criterion for the non-active sample was adjusted so that their mean absolute magnitude was roughly 10% fainter than the integrated Seyfert galaxy magnitude.) The advantage of using a CfA-selected sample (Huchra et al. 1983) is that it is believed to be spectroscopically complete to an apparent Zwicky magnitude of 14.5, permitting a reasonable matching

<sup>&</sup>lt;sup>2</sup>Papers I and II reported on 34 Seyfert galaxies, while only 32 are presented herein. This is because two of the Seyfert galaxies in this sample are strongly interacting, rendering the type of analysis presented in this paper highly problematic. As a result, these two systems were omitted from the discussion. This should not affect the basic conclusions.

of active and non-active galaxies and avoiding a number of possible sample biases. The disadvantage is that the sample size is relatively limited.

Each of the galaxies was observed in photometric conditions through a Cousins R filter using the f/7.5 0.9 m telescope at KPNO over the period 1991 May 16 – 24 UT. A Tektronix 2048 × 2048 CCD with 27  $\mu$ m pixels was used to record the data with a gain of 8.2 e<sup>-</sup> ADU<sup>-1</sup> and read-noise of 13 e<sup>-</sup>. The focal-plane scale was 0'.77 pixel<sup>-1</sup>. The target galaxy was exposed typically for 900 s, centered approximately in the unvignetted field of 21.9 × 26.8. The data were taken under seeing conditions of 1.4 – 3.0 arcseconds.

The data were reduced using the Image Reduction and Analysis Facility (IRAF)<sup>3</sup> and calibrated by means of Landolt (1992) standard fields in a straightforward manner.

It is important to note the advantages of CCD photometry compared with previous photographic surveys: in the first place, photometric accuracy is significantly better. This is important, not only for internal consistency among fields, but for quantitative comparisons with other studies, especially QSOs (see, e.g., Paper II). Secondly, the nucleus and disk are not saturated, permitting the search for companion systems and light asymmetries throughout the image, not just well outside the disk.

<sup>&</sup>lt;sup>3</sup>IRAF is distributed by the National Optical Astronomy Observatories, which are operated by the Association of Universities for Research in Astronomy, Inc., under cooperative agreement with the National Science Foundation.

# 3. REDUCTIONS AND ANALYSIS

### **3.1.** Surface Brightness Profiles and Structural Parameters

The apparent magnitudes of the host galaxies were measured in circular apertures with an appropriately sized sky-background annulus using the Picture Processing Package (PPP) of Yee (1991). The magnitudes typically converged to a couple of hundredths of a magnitude. Light from foreground stars was subtracted from the galaxy's integrated magnitude if the star was within the relevant aperture. The magnitudes were also corrected for Galactic absorption (as provided by the NASA/IPAC Extragalactic Database (NED)<sup>4</sup>, where  $A_R = 0.55 A_B$ ) when necessary.

One method of measuring the surface-brightness profiles of Seyfert galaxies is via a three-component, chi-squared minimization procedure (e.g., Alonso-Herrero, Ward, & Kotilainen 1996; and Kotilainen, Ward, & Williger 1993). That is, one could model the surface-brightness profile of a Seyfert galaxy by simultaneously modeling the nuclear, bulge, and disk components using appropriate fitting functions. This technique can be problematic, however, for data with a finite signal-to-noise (S/N) ratio, with relatively strong nuclear contamination of the bulge, leading to numerical instabilities and concerns about uniqueness.

One simplification is to ignore data within two seeing disks within the center of the galaxy (normally 5 pixels), and to then restrict the algorithm to a two-component fit—bulge plus disk—from which a nuclear contribution may be inferred.

<sup>&</sup>lt;sup>4</sup>The NASA/IPAC Extragalactic Database (NED) is operated by the Jet Propulsion Laboratory, California Institute of Technology, under contract with the National Aeronautics and Space Administration.

Experiments employing artificial data showed that while the disk parameters could be well recovered using either method, the bulge parameters showed a considerable degree of variability in some galaxies. Thus, both models have limited utility in this context.

A third technique adopts an empirical approach for modeling the nuclear component. Since Seyfert nuclei are point sources when they have distinct nuclei, (eg., Nelson et al. 1996; Malkan, Gorjian, & Tam 1998), it is reasonable to account for this component by subtracting a shifted profile of a scaled, high S/N ratio, unsaturated and unblended star near the host nucleus (i.e., a good point-spread function, PSF), using a scale factor based upon pre-determined fitting criteria. McLeod and Rieke (1995) used this latter technique in their analysis. They assumed the nuclear contribution to be that of a point source and then proceeded to subtract larger fractions of a PSF until the resulting profile started to turn over. We refer to this as the shift, scale, and subtract technique, or "SSS-technique." The resulting light distribution should then be virtually pure bulge + disk light and, hence, amenable to a 2-component fit. To be sure, this approach removes too much of the nuclear light, as artificial tests reveal, but so long as the fit ignores the inner 2 seeing disks, a reasonable two-component fit is produced for typical nuclear contributions. McLeod and Rieke (1995) obtained the same result; one achieves robust fits for a wide variety of nuclear brightnesses. The actual nuclear component is then found by subtracting the bulge and disk light calculated from the fitted structural parameters from the total light in the galaxy within some fiducial radius.

The IRAF/STSDAS Ellipse task was then used to generate the azimuthally averaged surface brightness profile with the nuclear component removed; that is, the intensity as a function of the semi-major axis (as well as ellipticity, position angle, ellipse center and ellipse harmonics) were computed along with the associated formal uncertainties.

The resulting surface-brightness profile was then modeled to determine the host-galaxy's

bulge and disk structural parameters using a two-component fit (see below) consisting of an  $r^{1/4}$  bulge (de Vaucouleurs 1948) and an exponential disk (Freeman 1970). Once the two structural parameters for each component were determined, a Gaussian PSF with the appropriate FWHM based on the seeing in the image was used to model the nucleus itself.

In linear units, it will be assumed that the intensity I of a Seyfert galaxy's profile at a radius r can be expressed:

$$I(r) = I_e e^{-7.688[(r/r_e)^{1/4} - 1]} + I_d e^{-r/r_o} + I_n e^{-r^2/2\sigma^2}$$
(1)

where the factors  $I_e$  and  $r_e$  are the intensity (at  $r_e$ ) and scale radius for the (de Vaucouleurs) bulge,  $I_d$  and  $r_o$  are the central intensity and scale radius for the (exponential) disk, while  $I_n$  and  $\sigma$  are the central intensity and standard deviation of the Gaussian PSF.

There are alternative functional forms for the bulge, but while a de Vaucouleurs law is not unique in its ability to fit the profiles of elliptical galaxies or bulges, the actual differences between it and other empirical laws are relatively small.

Virani & De Robertis (2000) utilize the structural parameters determined by fitting the surface brightness profile for each galaxy, as well as the nuclear component data, to search for intrinsic differences between Seyfert 1s and Seyfert 2s. The focus of this paper, however, is simply to compare the entire Seyfert population to the set of control galaxies.

The data were fit to Equation (1) using a robust non-linear least squares routine (Press et al. 1992). In this algorithm, the relative intensities for the bulge and disk,  $I_e$  and  $I_d$ , as well as the scale radii,  $r_e$  and  $r_o$ , are determined along with their formal uncertainties once the function's chi-squared achieves a global minimum. The reduced chi-squared is also reported. (Note that  $\sigma$  in Equation (1) is held constant.) The routine was tested at some length using artificial data sets representative of a galaxy with a pure bulge, with a pure disk, with a bulge and disk in varying proportions, and with the addition of a nuclear

component of various strengths. In all cases we found good agreement between the code's results and the input data parameters. Moreover, the routine was designed so that data from the innermost pixels (roughly equivalent to two seeing disks) were not used. This provided us with the additional assurance that we were fitting a bulge plus disk light profile and further mitigated the small contribution from any remaining nuclear component. The efficacy and accuracy of our computer algorithm is more thoroughly explored and discussed in Virani & De Robertis (2000).

The results of this analysis are recorded in Tables 1-6. Table 1 lists the structural parameters with their formal uncertainty for the control sample;  $r_o$  and  $r_e$  are the scale radii for the disk and bulge respectively, while  $\mu_d$  and  $\mu_b$  are the appropriate surface brightnesses corresponding to  $I_d$  and  $I_e$ . Table 2 shows the fraction of light in the bulge and disk for each system, the bulge-to-disk ratio (B/D), as well as the total (integrated) apparent R magnitude for each galaxy in the control sample. Tables 3 and 4 give the structural parameters for the Seyfert 1s and 2s respectively, while Tables 5 and 6 show the fraction of light in each of the three components: disk, bulge and nuclear, as well as the their bulge-to-disk ratio and integrated R magnitude.

Figure 1 shows the distribution of the disk scale radius (top) and bulge scale radius for radii less than 7 kpc. (While there are scale radii larger then 7 kpc, these also contain proportionally very large uncertainties.) The solid line shows the control sample, while the dashed line is for the Seyfert galaxies (types 1 and 2s together). Figure 2 shows the distribution of disk (top) and bulge (bottom) surface brightnesses. Figure 3 illustrates the distribution of the bulge-to-disk ratios. Kolmogorov-Smirnov (K-S) tests show that there are no significant differences between the control and active samples in these structural parameters.

### **3.2.** Companion Galaxy Characteristics

Unlike Paper I in which object classification and analysis were performed entirely using PPP, all non-stellar objects within a projected radius of  $200 \, h^{-1}$  kpc were identified using both visual inspection and the shape of the light profile compared with a local stellar profile. There was excellent agreement between the sample of companion galaxies detected in an automated fashion with PPP with those detected manually. By adding artificial companion galaxies to a variety of real Seyfert host galaxies, it was determined that typically galaxies brighter than  $R \approx +18.5$  (corresponding to an absolute magnitude of  $M_R \approx -16.5$ , slightly fainter than the SMC at the mean redshift of the sample) could be recovered outside the immediate nucleus.

A search for companion galaxies and light asymmetries projected on the disk of a host galaxy was performed using unsharp masking techniques. That is, the data were convolved using a flux-preserving Gaussian kernel with a full-width at half-maximum (FWHM) equal to four times the seeing. The original image was then divided by the convolved image to yield an "unsharp-masked" image. Light asymmetries are more readily identified in the masked image and can be classified in a qualitative sense as either spiral arms, bars, rings, isophotal twisting and/or very close companion galaxy.

The instrumental magnitude and position of each companion galaxy relative to the nucleus of the host galaxy were measured. These were converted to an apparent magnitude and projected separation using the photometric calibration and redshift of the host galaxy under the assumption that the companion lies at the same distance as the host. Figure 4a provides a histogram of the distribution of apparent magnitudes for the relevant samples, while Figure 4b shows the corresponding absolute magnitude distributions under the assumption that the companion galaxies are situated at the same redshift as the host.

All histograms follow the same format: the solid line indicates the control sample,

while the dashed line shows the Seyfert sample (1s and 2s combined). The histograms have been normalized such that the area under each curve is unity. Quantitative comparisons between distributions using the K-S test in which the *null hypothesis* is that the two data sets (properties) being compared are from the same underlying population. Differences are significant only when the K-S test rejects the null hypothesis at a confidence level of 95% or greater. The results from the K-S test on both distributions show that the null hypothesis cannot be rejected, apart from a marginal agreement between the central bulge surface brightnesses,  $\mu_b$ , of the control sample and Seyfert 2s.

Within a projected radius of 200 kpc, 359 optical companions were found around the 32 Seyfert host galaxies for a companion frequency of  $11.2 \pm 1.0$  companions/host (175 around Seyfert 1 and 184 around Seyfert 2), and 520 optical companions were found around the 47 control host galaxies for a companion frequency of  $10.6 \pm 0.9$  companions/host (where the uncertainties are the root-mean-square of the mean). Figure 5 shows the relative frequency of the number of companions around each host. The K-S test indicates that the distributions are similar for the two samples.

Figure 6 illustrates the distribution of projected separations, s, between the centers of a host and companion, assuming they are situated at the same distance. While the K-S test suggests that both distributions are similar, the Seyfert sample has a marginally higher companion frequency within 50 kpc. Figure 7 depicts the distribution of position angles of companion galaxies with respect to the host galaxy. The histogram is binned into  $45^{\circ}$  intervals. The observed distributions are consistent with a uniform random distribution as might be expected. Figure 8 shows the distribution of the logarithm of the magnitude difference between the host and companion galaxies, assuming once again that the companions lie at the same distance as the host. Note that at  $R \approx +19$  the distribution turns over and rapidly drops to zero, indicating the limiting magnitude to

which companions could be detected efficiently.

The maximum tidal influence of a companion galaxy on its host galaxy,  $Q_i$ , is proportional to the companion's mass divided by the cube of its projected separation,  $s_i$ . Under the assumption that light traces mass and that the companions are situated at the redshift of the host, then the maximum tidal parameter for each host  $Q \propto \sum_{i=1}^{N} Q_i$  where  $Q_i \propto L_i/s_i^3$  and  $L_i$  is the luminosity of the companion. Figure 9 indicates the distribution of this parameter. A K-S test shows that the distribution of this tidal parameter is similar for both the Seyfert and control samples. Moreover, Seyfert 1s and 2s have similar tidal parameter distributions. There are a few hosts in both samples for which  $Q > 10^5 L^*/\mathrm{Mpc}^3$  implying severely disturbed systems. ( $L^*$  here is the equivalent luminosity for an  $M_R^* = -22.1$  galaxy; Schechter 1976.)

As with all the parameters related to the optical companions of the host galaxies, the environments of Seyfert galaxies and the control galaxies are very similar. There is a difference in the distribution of faint galaxies around Seyfert 1s compared with Seyfert 2s, though when considered together, the Seyfert and a non-active (control) companion distributions are similar. There is also no obvious difference in the tidal influences the companion galaxies have on the hosts, though both samples have their share of very tidally disturbed systems ( $\sim 8\%$ ).

#### 3.2.1. Host Galaxy Light Asymmetries

Light asymmetries and morphological disturbances with host galaxies are important features to consider since they *may* be a symptom of a recent interaction or merger or evidence for a radial flow of material. Though such features can only be characterized in a qualitative sense, it might be expected that a sample of active galaxies would show a

greater departure from "normalcy" than a non-active sample; i.e., from typical exponential (spiral) disks and featureless bulges.

Using primarily the unsharp masking technique, each host galaxy was searched for the following features: bars, rings, significant isophotal twisting, and other features that could be evidence for a recent interaction: e.g., tidal tails, bridges, and (asymmetric) prominent dust lanes.

Bars have long been considered an efficient mechanism for transporting gas to the sub-kpc regions of a galaxy, and hence, an AGN (e.g., Athanassoula 1992; Shlosman & Noguchi 1993). Inner and outer rings are also formed during "disturbances" (e.g., Hunt & Malkan 1999) or when a companion galaxy passes right through the host galaxy (e.g., Combes et al.1991). Other distortions may also provide circumstantial evidence for a recent interaction such as tidal tails, bridges, prominent dust lanes, or other significant light asymmetries. Similarly, an extreme twisting of isophotes, where the position angle well outside the nucleus changes by a large amount, in this case  $\pm 45^{\circ}$ , could also flag a previous disturbance.

Tables 7 and 8 show the frequency of such morphological disturbances in both the Seyfert host and the control host respectively detected in this analysis. A ( $\blacktriangle$ ) indicates that the feature was noticed in the galaxy, and ( $\triangle$ ) indicates that only a partial feature was observed. Column 1 gives the name of the galaxy, columns 2 – 5 indicate a Bar, Ring, Distortion, or large Position-Angle excursion for each system respectively, while column 6 shows the occurrence of any of the previous disturbances (i.e. bar and/or ring and/or distortions).

Table 9 summarizes the frequency of bars, rings, and other distortions. It presents the number of galaxies containing the feature (including partial features in parentheses) as well as the percentage of galaxies with that feature. As can be seen, there are slightly different

ratios of galaxies that contain bars or rings in both samples. However, a large fraction of galaxies in both samples contain some form of disturbance, although a slightly larger fraction of Seyfert galaxies contain a disturbance.

Acknowledging the qualitative nature of this classification, there do not appear to be large differences between the active and non-active samples. Certainly there are no differences in the frequency of bars and "distortions." Seyfert galaxies may have rings somewhat more frequently and exhibit large position-angle excursions, but the significance is marginal at best. It appears that in terms of light asymmetries and disturbances, Seyfert galaxy hosts are not significantly different from the hosts of the non-active sample.

In a naive interpretation of the interaction or merger hypothesis for active galaxies, differences within the local environments and perhaps even host-galaxy properties might be expected between Seyfert galaxies and a reasonably matched control sample. At the level of investigation presented in this paper, however, no statistically significant differences are uncovered. When combined with the analyses presented in Papers I and II, it appears that if the interaction/merger model is correct, then its interpretation must be more complex than imagined.

## 4. CONCLUSION

A technique was developed that allowed the measurement of the structural parameters of the bulge and disk in the hosts in a sample of Seyfert and control (non-active) galaxies. No statistically significant differences were found in these parameters according to the K-S test.

A comparison between the properties of the companion galaxies within 200  $h^{-1}$  kpc of each host in both the active and control samples — i.e., the distributions of apparent R

magnitude, absolute R magnitude (assuming the "companions" are at the distance of the host), projected separation from the host, position angle relative to the host, magnitude difference between the companion and host, and strength of the tidal parameter — show no statistically significant differences.

Moreover, no statistically significant differences were found between the control and active sample host galaxies in terms of light asymmetries — bars, rings, isophotal twisting, etc.

It appears that the nearby environment of Seyfert galaxies is not significantly different from non-active galaxies with the same morphological distribution; that is, the companion characteristics are indistinguishable, as are the structural parameters and a qualitative assessment of any light asymmetries.

Differences in some of these properties might have been anticipated according to a simple interpretation of the interaction or merger hypothesis for the initiation of activity in galactic nuclei. That none was found may indicate that if this hypothesis is correct, it must be operating on a more complex level.

The analyses presented in this paper are largely the result of MSc theses by VanDalfsen (1997) and Virani (2000). M.M.D.R. gratefully acknowledges financial support by the Natural Sciences and Engineering Research Council of Canada on which this research was based.

#### REFERENCES

Alonso-Herrero, A., Ward, M.J., & Kotilainen, J.K. 1996, MNRAS, 278, 902

Athanassoula, E. 1992, MNRAS, 259, 345

Combes, F., Boissé, P., Mazure, A., & Blanchard, A. 1991, In Galaxies and Cosmology, Springer-Verlag.

De Robertis, M.M., Hayhoe, K., & Yee, H.K.C. 1998a, ApJS, 115, 163 (Paper I)

De Robertis, M.M., Yee, H.K.C., & Hayhoe, K. 1998b, ApJ, 496, 93 (Paper II)

de Vaucouleurs, G. 1948, Ann. d'Astrophys., 11, 247

Dultzin-Hacyan, D., Krongold, Y., Fuentes-Guridi, I., & Marziani, P. 1999a, ApJ, 513, 111

Freeman, K. 1970, ApJ, 160, 811

Huchra, J., Davis, M., Latham, D., & Tonry, J. 1983, ApJS, 52, 82

Hunt, L.K., & Malkan, M.A. 1999, ApJ, 516, 660

Keel, W.C. 1996, AJ, 111, 696

Kelm, B., Focardi, P., & Palumbo, G.G.C. 1998, A&A, 335, 912

Kotilainen, J., Ward, M.J., & Williger, G. 1993, MNRAS, 263, 655

Landolt, A. 1992, AJ, 104, 340

Laurikainen, E., & Salo, H. 1995, A&A, 293, 683

Laurikainen, E., Salo, H., Teerikorpi, P., & Petrov, G. 1994, A&AS, 108, 491

Malkan, M.A., Gorjian, V., & Tam, R. 1998, ApJS, 117, 25

McLeod, K., & Rieke, G. 1995, ApJ, 441, 96

Mulchaey, J.S., & Regan, M.W. 1997, ApJ, 482, 135

Mulchaey, J.S., Regan, M.W., & Kundu, A. 1997, ApJS, 110, 299

Nelson, C.H., Mackenty, J.W., Simkin, S.M., & Griffiths, R.E. 1996, ApJ, 466, 713

Press, W., Flannery, B., Teudolsky, S., & Vetterling, W. 1992. Numerical Recipes in FORTRAN: The Art of Scientific Computing (2 ed.) Cambridge University Press.

Schechter, P. 1976, ApJ, 203, 297

Shlosman, I., & Noguchi, M. 1993, ApJ, 414, 474

VanDalfsen, M. 1997. MSc Thesis. The Nearby Environment of Seyfert Galaxies: A comparative Study

Virani, S. 1999. MSc Thesis. In preparation.

Yee, H.K.C. 1991. PASP, 103, 396

This manuscript was prepared with the AAS  $\LaTeX$  macros v5.0.

- Fig. 1.— Relative distribution of disk scale lengths (top) and bulge scale lengths (bottom) for radii less than 7 kpc. Control galaxies are shown with a solid line, while Seyfert galaxies (1s and 2s) by a dashed line hereafter.
- Fig. 2.— Relative distribution of disk central surface brightnesses (top) and bulge central surface brightnesses (bottom).
- Fig. 3.— Relative distribution of bulge-to-disk ratios for control galaxies (solid line) and Seyfert galaxies (dashed line) for ratios less than 2.
- Fig. 4.— Relative distribution of R apparent magnitudes (top) and R absolute magnitudes (bottom) of companion galaxies within a projected radius of 200 kpc of the main galaxy. In the latter case, the companion galaxies are assumed to have the same distance as the main galaxy.
- Fig. 5.— Relative distribution of the number of companion galaxies within 200 kpc of the main galaxy.
- Fig. 6.— Relative distribution of the projected separation of companion galaxies from the main galaxy for distances less than 200 kpc.
- Fig. 7.— Relative distribution of the position angle of the companion galaxies with respect to the main galaxy for distances less than 200 kpc.
- Fig. 8.— Relative distribution of the difference in R apparent magnitude between the companion galaxy and the host or main galaxy for companions less than 200 kpc.
- Fig. 9.— Relative distribution of the tidal strength of companion galaxies surrounding the host or main galaxy for companions less than 200 kpc.

Table 1. Surface-Brightness Profile Parameters Of The Control Galaxies

	$r_o$	$r_e$	$\mu_d$	$\mu_b$	
Name	(kpc)	(kpc)	$(\text{mag}/\epsilon$	$arcsec^2$ )	$\chi^2_{\nu}$
IC 875	$3.6 \pm 0.1$	$2.1 \pm 0.1$	$20.88 \pm 0.09$	$20.38 \pm 0.07$	0.606
IC 1141	$1.9 \pm 0.0$	$0.5 \pm 0.1$	$18.81 \pm 0.08$	$17.66 \pm 0.42$	1.132
NGC 3169	$0.5 \pm 0.0$	$12.7 \pm 0.6$	$16.54 \pm 0.04$	$22.51 \pm 0.09$	0.688
NGC 3756	$4.7 \pm 0.1$	$1.4 \pm 0.1$	$20.05 \pm 0.02$	$22.87 \pm 0.13$	2.453
NGC 3825	$14.7 \pm 1.1$	$3.7 \pm 0.1$	$21.80 \pm 0.11$	$19.67\pm0.06$	6.402
NGC 3938	$6.4 \pm 0.7$	$9.0 \pm 0.4$	$21.56 \pm 0.13$	$21.66 \pm 0.01$	3.512
NGC 3968	$15.5 \pm 0.5$	$4.7 \pm 0.2$	$20.46 \pm 0.05$	$20.69 \pm 0.07$	1.372
NGC 4045	$6.9 \pm 0.4$	$3.2 \pm 0.2$	$21.36 \pm 0.11$	$21.23 \pm 0.08$	2.402
NGC 4048	$2.3 \pm 0.0$		$18.31 \pm 0.01$		5.230
NGC 4088	$1.1 \pm 0.0$		$18.35 \pm 0.02$	•••	3.651
NGC 4172	$2.3 \pm 0.0$	$25.8 \pm 1.0$	$18.77 \pm 0.10$	$22.62 \pm 0.08$	3.131
NGC 4224	$6.6 \pm 0.1$	$6.9 \pm 0.3$	$20.05 \pm 0.05$	$21.73 \pm 0.05$	0.603
NGC 4352	$0.9 \pm 0.0$	$15.7 \pm 0.3$	$19.27 \pm 0.05$	$23.49 \pm 0.04$	6.485
NGC 4375	$8.7 \pm 0.1$	$7.4 \pm 0.9$	$19.73 \pm 0.05$	$21.89 \pm 0.16$	3.438
NGC 4477	$0.4 \pm 0.0$	$7.4 \pm 0.1$	$17.51 \pm 0.05$	$21.62 \pm 0.04$	4.706
NGC 4799	$1.9 \pm 0.0$	$6.1 \pm 0.7$	$18.14 \pm 0.02$	$22.84 \pm 0.13$	1.113
NGC 4944	$5.1 \pm 0.1$		$18.04 \pm 0.01$		1.791
NGC 4954	$4.4 \pm 0.0$	$39.9 \pm 12.7$	$18.14 \pm 0.03$	$25.44 \pm 0.51$	3.705
NGC 5289	$5.7 \pm 0.2$	$1.5 \pm 0.1$	$20.67 \pm 0.06$	$19.47 \pm 0.08$	4.261

Table 1—Continued

	$r_o$	$r_e$	$\mu_d$	$\mu_b$	
Name	(kpc)	(kpc)	$(\text{mag}/\epsilon$	$\operatorname{arcsec}^2)$	$\chi^2_{ u}$
NGC 5375	$5.1 \pm 0.5$	$8.7 \pm 0.6$	$21.73 \pm 0.39$	$22.39 \pm 0.07$	1.121
NGC 5505	$2.6 \pm 0.0$	• • •	$18.78 \pm 0.01$	• • •	2.227
NGC 5515	$4.2 \pm 0.2$	$11.9 \pm 0.6$	$19.51 \pm 0.09$	$21.92 \pm 0.10$	1.016
NGC 5541	$6.0 \pm 0.2$	$0.6 \pm 0.3$	$18.62 \pm 0.04$	$18.20\pm1.25$	1.832
NGC 5603	$1.1 \pm 0.0$	$5.9 \pm 0.2$	$18.08 \pm 0.06$	$21.15 \pm 0.05$	1.926
NGC 5644	$22.1 \pm 3.8$	$7.3 \pm 0.2$	$23.00 \pm 0.24$	$20.50 \pm 0.03$	2.833
NGC 5772	$8.3 \pm 0.1$	$1.6 \pm 0.0$	$19.94 \pm 0.02$	$19.21\pm0.05$	7.402
NGC 5806	$3.4 \pm 0.0$	$1.1\pm0.1$	$19.44 \pm 0.03$	$20.43 \pm 0.01$	6.070
NGC 5876	$11.2 \pm 0.5$	$3.8 \pm 0.1$	$21.53 \pm 0.08$	$20.47 \pm 0.04$	5.131
NGC 5908	$5.1 \pm 0.1$	$7.5 \pm 2.4$	$18.43 \pm 0.05$	$22.29 \pm 0.31$	0.186
NGC 5957	$3.3 \pm 0.0$	$1.9 \pm 0.2$	$20.00 \pm 0.03$	$21.81 \pm 0.11$	2.397
NGC 5980	$4.3 \pm 0.1$	$8.1 \pm 2.4$	$18.65 \pm 0.03$	$23.17 \pm 1.09$	0.876
NGC 6001	$8.6 \pm 0.2$	$0.4 \pm 0.1$	$19.80 \pm 0.02$	$15.85 \pm 0.43$	1.037
NGC 6014	$2.9 \pm 0.0$	$0.8 \pm 0.1$	$19.76 \pm 0.03$	$20.06 \pm 0.18$	2.293
NGC 6030	$3.0 \pm 0.0$	$6.2 \pm 0.2$	$19.43 \pm 0.03$	$21.34 \pm 0.04$	2.885
NGC 6085		$12.0 \pm 0.1$		$21.35 \pm 0.02$	6.148
NGC 6111	$1.6 \pm 0.0$	$7.5 \pm 0.8$	$18.79 \pm 0.03$	$23.36 \pm 0.12$	0.483
NGC 6126	$21.3 \pm 2.0$	$8.0 \pm 0.3$	$22.57 \pm 0.16$	$21.16 \pm 0.05$	0.287
NGC 6143	$4.9 \pm 0.1$	$2.4 \pm 0.7$	$19.84 \pm 0.04$	$22.49 \pm 0.40$	3.291

Table 1—Continued

	$r_o$	$r_e$	$\mu_d$	$\mu_b$	
Name	(kpc)	(kpc)	(mag/a)	$arcsec^2$ )	$\chi^2_{ u}$
NGC 6155	$2.5 \pm 0.0$	$0.3 \pm 0.1$	$19.16 \pm 0.02$	$19.47\pm0.74$	2.247
NGC 6197		$10.1 \pm 0.1$	• • •	$20.67 \pm 0.02$	2.527
NGC 6764	$12.7 \pm 0.5$	$0.5 \pm 0.0$	$20.41 \pm 0.02$	$18.55 \pm 0.13$	0.388
UGC 05734	$1.7 \pm 0.0$	$30.0 \pm 3.2$	$17.25 \pm 0.05$	$23.34 \pm 0.19$	0.586
UGC 07064	$4.6 \pm 0.1$	$0.9 \pm 0.9$	$19.05 \pm 0.05$	$18.02 \pm 0.31$	4.418
UGC 09295	$2.9 \pm 0.0$		$17.69 \pm 0.01$	• • •	7.650
UGC 10097	$7.8 \pm 0.2$	$3.2 \pm 0.1$	$20.45 \pm 0.06$	$19.52 \pm 0.05$	1.626
UGC 11865	$2.0 \pm 0.0$	$12.4 \pm 5.9$	$17.39 \pm 0.06$	$23.83 \pm 1.01$	0.239
Means	$5.6 \pm 0.1$	$7.3 \pm 0.4$	$19.50 \pm 0.01$	$21.13 \pm 0.06$	2.74

Table 1. Galactic Light Distribution And Magnitudes Of Control Galaxies

	$f_b$	$f_d$		$m_b$	$m_d$
Name	(%)	(%)	$\mathrm{B}/\mathrm{D}$	(mag)	(mag)
IC 875	66.6	33.4	1.998	12.65	13.41
IC 1141	42.4	57.6	0.735	13.90	13.56
NGC 3169	81.3	18.7	4.339	10.01	11.60
NGC 3756	2.9	97.1	0.030	14.27	10.46
NGC 3825	72.9	27.1	2.697	12.42	13.50
NGC 3938	60.5	39.5	1.529	8.82	11.21
NGC 3968	27.9	72.1	0.387	12.88	11.85
NGC 4045	55.9	44.1	1.267	11.80	12.06
NGC 4048		100	0.000		12.79
NGC 4088		100	0.000		10.92
NGC 4172	88.4	11.6	7.634	12.44	14.65
NGC 4224	44.1	55.9	0.789	11.34	11.08
NGC 4352	91.6	8.4	10.856	11.53	14.12
NGC 4375	25.8	74.2	0.348	13.93	12.78
NGC 4477	93.9	6.1	15.440	9.88	12.85
NGC 4799	25.2	74.8	0.337	13.05	11.87
NGC 4944		100	0.000		11.66
NGC 4954	13.7	86.3	0.158	14.57	12.57
NGC 5289	46.3	53.7	0.861	12.21	12.04

Table 1—Continued

	$f_b$	$f_d$		$m_b$	$m_d$
Name	(%)	(%)	$\mathrm{B}/\mathrm{D}$	(mag)	(mag)
NGC 5375	83.7	16.3	5.125	11.86	13.77
NGC 5505		100	0.000	• • •	12.76
NGC 5515	71.2	28.8	2.468	12.65	13.64
NGC 5541	4.8	95.2	0.051	15.34	12.11
NGC 5603	84.7	15.3	5.546	12.68	14.54
NGC 5644	88.4	11.6	7.652	12.19	14.39
NGC 5772	23.4	76.6	0.305	13.10	11.81
NGC 5806	16.7	83.3	0.200	12.38	10.63
NGC 5876	63.2	36.8	1.721	11.80	12.39
NGC 5908	16.0	84.0	0.191	12.25	10.45
NGC 5957	19.0	81.0	0.234	13.36	11.79
NGC 5980	13.6	86.4	0.157	13.47	11.46
NGC 6001	21.3	78.7	0.271	14.49	13.07
NGC 6014	19.0	81.0	0.235	14.01	12.43
NGC 6030	68.7	31.3	2.193	12.39	13.24
NGC 6085	100			12.63	
NGC 6111	40.1	59.9	0.670	13.40	12.97
NGC 6126	74.3	25.7	2.888	13.14	14.30
NGC 6143	7.2	92.8	0.078	15.76	13.00

Table 1—Continued

	$f_b$	$f_d$		$m_b$	$m_d$
Name	(%)	(%)	$\mathrm{B}/\mathrm{D}$	(mag)	(mag)
NGC 6155	3.2	96.8	0.033	15.75	12.03
NGC 6197	100			12.11	
NGC 6764	9.4	90.6	0.104	13.37	10.92
UGC 05734	66.3	33.7	1.971	12.42	13.16
UGC 07064	25.5	74.5	0.342	14.18	13.01
UGC 09295		100	0.000		13.09
UGC 10097	60.9	39.1	1.560	12.38	12.86
UGC 11865	18.7	81.3	0.230	15.17	13.57
Means	44.6	55.4	2.144	12.88	12.55

Table 1. Surface-Brightness Profile Parameters of Seyfert 1 Galaxies

	$r_o$	$r_e$	$\mu_d$	$\mu_b$	
Name	(kpc)	(kpc)	(mag/a)	$arcsec^2$ )	$\chi^2_{ u}$
Mrk 231	$12.3 \pm 1.9$	$1.4 \pm 0.2$	$20.95 \pm 0.26$	$16.68 \pm 0.29$	0.497
Mrk 789	$1.6 \pm 0.1$	$5.1 \pm 6.1$	$17.38 \pm 0.24$	$22.32 \pm 2.32$	0.574
Mrk 817	$3.7 \pm 0.1$	$6.4 \pm 3.8$	$18.80 \pm 0.06$	$22.77 \pm 0.69$	3.715
Mrk 841	$7.9 \pm 1.9$	$1.5 \pm 0.3$	$22.39 \pm 0.59$	$18.72 \pm 0.50$	0.170
NGC 3080	$4.2 \pm 0.3$	$17.4 \pm 2.6$	$20.16 \pm 0.11$	$23.42 \pm 0.21$	1.014
NGC 3227	$4.4 \pm 0.1$	$0.7 \pm 0.1$	$19.39 \pm 0.03$	$19.59 \pm 0.30$	0.233
NGC 3516	$8.2 \pm 1.0$	$1.9 \pm 0.1$	$21.90 \pm 0.21$	$19.20 \pm 0.09$	1.587
NGC 3718	$4.2\pm0.1$	$1.7 \pm 0.3$	$20.38 \pm 0.06$	$21.75 \pm 0.24$	0.165
NGC 4051	$5.2 \pm 0.2$	$0.9 \pm 0.1$	$20.63 \pm 0.03$	$21.28 \pm 0.10$	1.244
NGC 4151	$8.5 \pm 0.5$	$0.8 \pm 0.1$	$21.49 \pm 0.05$	$19.34 \pm 0.08$	3.027
NGC 4235	$10.8 \pm 0.3$	$13.0 \pm 2.1$	$20.61 \pm 0.14$	$22.36 \pm 0.18$	0.377
NGC 4253	$2.1\pm0.1$	$4.0\pm1.0$	$18.57 \pm 0.07$	$22.08 \pm 0.44$	0.677
NGC 5548	$10.3 \pm 0.6$	$2.8 \pm 0.3$	$21.29 \pm 0.13$	$19.79 \pm 0.18$	1.071
NGC 5940	$7.1 \pm 0.2$	$0.4 \pm 0.2$	$19.74 \pm 0.05$	$17.33 \pm 0.97$	1.727
NGC 6814	$4.2 \pm 0.1$	$2.4 \pm 0.2$	$20.06 \pm 0.06$	$21.57 \pm 0.12$	0.685
Means	$6.3 \pm 0.2$	$4.0 \pm 0.5$	$20.25 \pm 0.05$	$20.55 \pm 0.18$	1.117

 ${\it Table 1.} \quad {\it Surface-Brightness Profile Parameters of Seyfert 2 Galaxies}$ 

	$r_o$	$r_e$	$\mu_d$	$\mu_b$	
Name	(kpc)	(kpc)	•	$arcsec^2$ )	$\chi^2_ u$
Mrk 461	$3.3 \pm 0.1$	$0.9 \pm 0.1$	$19.63 \pm 0.06$	$19.10 \pm 0.31$	2.984
Mrk 471	$3.2 \pm 0.1$	$40.7 \pm 22.0$	$18.61 \pm 0.17$	$24.52 \pm 0.94$	1.012
NGC 3362	$7.9 \pm 0.3$	$3.0 \pm 1.1$	$19.67\pm0.07$	$21.88 \pm 0.53$	1.221
NGC 3786	$4.1\pm0.1$	$0.4 \pm 0.1$	$19.82 \pm 0.03$	$18.28 \pm 0.45$	2.094
NGC 3982	$1.4 \pm 0.1$	$0.9 \pm 0.2$	$19.05 \pm 0.10$	$20.97 \pm 0.32$	2.852
NGC 4388	$7.2 \pm 0.4$	$50.1 \pm 19.0$	$19.25 \pm 0.05$	$24.57 \pm 0.28$	0.254
NGC 5252	$5.4 \pm 0.3$	$13.6 \pm 1.6$	$19.98 \pm 0.08$	$22.26 \pm 0.13$	0.156
NGC 5273	$3.0 \pm 0.1$	$1.3\pm0.1$	$20.75 \pm 0.04$	$21.43 \pm 0.06$	1.296
NGC 5283	$5.7 \pm 1.5$	$1.1\pm0.1$	$23.07 \pm 0.35$	$19.99 \pm 0.10$	1.285
NGC 5347	$5.3 \pm 0.3$	$2.1 \pm 0.3$	$20.60 \pm 0.08$	$21.58 \pm 0.21$	1.408
NGC 5674	$8.3 \pm 0.4$	$4.1 \pm 2.0$	$20.26 \pm 0.23$	$20.74 \pm 0.78$	2.783
NGC 5695	$3.5 \pm 0.1$	$0.7 \pm 0.1$	$19.10 \pm 0.04$	$18.80 \pm 0.42$	1.169
NGC 5929		$3.7 \pm 0.1$		$21.21 \pm 0.06$	0.451
UGC 06100	$4.2 \pm 0.3$	$21.6 \pm 2.8$	$20.03 \pm 0.13$	$23.37 \pm 0.19$	0.572
UGC 08621	$3.0 \pm 0.1$	$0.3 \pm 0.2$	$18.67 \pm 0.02$	$18.55 \pm 1.32$	0.596
Means	$4.7 \pm 0.1$	$9.6 \pm 2.0$	$19.89 \pm 0.04$	$21.15 \pm 0.14$	1.342

Table 1. Galactic Light Distribution And Magnitudes of Seyfert 1 Galaxies

	$f_n$	$f_d$	$f_b$		$m_{ m nuc}$	$m_d$	$m_b$
Name	(%)	(%)	(%)	B/D	(mag)	(mag)	(mag)
Mrk 231	9.2	21.8	69.0	3.162	15.12	12.93	14.18
Mrk 789	1.8	76.1	22.2	0.291	18.15	15.40	14.06
Mrk 817	25.3	60.8	13.9	0.228	14.63	15.28	13.67
Mrk 841	37.5	9.7	52.8	5.442	14.82	14.44	16.28
NGC 3080	2.4	33.6	64.0	1.902	17.87	14.31	15.00
NGC 3227	2.8	87.6	9.5	0.109	13.62	12.31	9.90
NGC 3516	0.2	19.0	80.8	4.265	17.98	11.52	13.09
NGC 3718	0.1	82.7	17.2	0.208	18.45	12.18	10.48
NGC 4051	1.9	87.3	10.8	0.124	14.25	12.33	10.06
NGC 4151	8.1	51.3	40.6	0.790	13.09	11.34	11.09
NGC 4235	0.1	48.8	51.1	1.049	17.44	10.62	10.67
NGC 4253	13.3	61.8	24.9	0.403	14.40	13.72	12.73
NGC 5548	10.4	39.0	50.7	1.300	14.61	12.89	13.18
NGC 5940	5.1	82.7	12.2	0.148	16.65	15.70	13.62
NGC 6814	0.2	74.2	25.6	0.345	17.33	12.26	11.10
Means	7.9	55.8	36.4	1.318	15.89	12.61	13.15

Table 1. Galactic Light Distribution And Magnitudes Of Seyfert 2 Galaxies

	c	c	c				
	$f_n$	$f_d$	$f_b$		$m_{ m nuc}$	$m_d$	$m_b$
Name	(%)	(%)	(%)	$\mathrm{B}/\mathrm{D}$	(mag)	(mag)	(mag)
Mrk 461	0.1	68.3	31.7	0.464	22.46	14.30	13.47
Mrk 471	0.1	50.5	49.5	0.980	21.14	13.96	13.93
NGC 3362	1.0	92.2	6.8	0.073	17.63	15.56	12.72
NGC 3786	0.8	84.3	14.9	0.177	17.07	13.84	11.96
NGC 3982	0.1	81.4	18.6	0.229	20.08	13.07	11.47
NGC 4388	0.1	66.1	33.9	0.512	19.16	10.69	9.96
NGC 5252	0.3	31.0	68.7	2.219	18.30	12.51	13.37
NGC 5273	0.1	68.6	31.3	0.457	18.85	12.60	11.75
NGC 5283	2.7	14.7	82.7	5.638	16.65	12.93	14.80
NGC 5347	0.3	75.6	24.1	0.319	18.32	13.48	12.24
NGC 5674	1.2	61.7	37.1	0.601	17.32	13.56	13.01
NGC 5695	1.1	83.4	15.5	0.185	17.13	14.24	12.41
NGC 5929	2.2		97.8		16.54	12.40	
UGC 06100	3.7	27.9	68.4	2.450	16.66	13.48	14.45
UGC 08621	0.6	95.6	3.6	0.037	18.50	16.63	13.06
Means	1.0	64.4	39.0	1.024	18.39	12.76	13.55

Table 1. Bars, Rings and Distortions: Seyfert Hosts

Name	Bar	Ring	Dis	P.A.	Any
Mrk 231			<b>A</b>	<b>A</b>	<b>A</b>
Mrk 461	<b>A</b>				<b>A</b>
Mrk 471	<b>A</b>			•	•
Mrk 789			<b>A</b>		•
Mrk 817					
Mrk 841					
UGC 06100	Δ				Δ
UGC 08621				<b>A</b>	<b>A</b>
NGC 3080				<b>A</b>	<b>A</b>
NGC 3227			<b>A</b>		<b>A</b>
NGC 3362				<b>A</b>	<b>A</b>
NGC 3516				•	•
NGC 3718			Δ	•	•
NGC 3786		Δ	<b>A</b>		•
NGC 3982			Δ	•	•
NGC 4051			<b>A</b>		•
NGC 4151	<b>A</b>	Δ		•	<b>A</b>
NGC 4235			Δ		Δ
NGC 4253	<b>A</b>	Δ			<b>A</b>
NGC 4388			Δ		Δ

Table 1—Continued

Name	Bar	Ring	Dis	P.A.	Any
NGC 5252					
NGC 5256			<b>A</b>		<b>A</b>
NGC 5273					
NGC 5283					
NGC 5347	<b>A</b>	<b>A</b>			<b>A</b>
NGC 5548		<b>A</b>	<b>A</b>	•	<b>A</b>
NGC 5674	<b>A</b>	<b>A</b>			<b>A</b>
NGC 5695	Δ				Δ
NGC 5929					
NGC 5940	<b>A</b>				<b>A</b>
NGC 6104		<b>A</b>	<b>A</b>		<b>A</b>
NGC 6814	Δ	Δ			Δ

Table 1. Bars, Rings and Distortions: Control Hosts

UGC 05734 △ △ NGC 4954 UGC 07064 ▲ ▲ MGC 5289 ▲ ▲ UGC 09295 NGC 5375 ▲			
UGC 07064 ▲ ▲ NGC 5289 ▲ ▲			
HCC 00205 NCC 5375 ▲			<b>A</b>
11GC 9979 A			<b>A</b>
UGC 10097 NGC 5505 ▲			<b>A</b>
UGC 10407 $\blacktriangle$ NGC 5515 $\triangle$			Δ
UGC 11865 ▲ NGC 5541	<b>A</b>		<b>A</b>
IC 875 NGC 5603			
IC 1141 NGC 5644			
NGC 3169 ▲ NGC 5690	<b>A</b>		•
NGC 3492 ▲ NGC 5772			
NGC 3756 NGC 5806 $\triangle$			Δ
NGC 3825 ▲		<b>A</b>	•
NGC 3938	Δ		Δ
NGC 3968 ▲			<b>A</b>
NGC 4045 △ <b>▲ ▲</b> NGC 5980			
NGC 4048 ▲ ▲ NGC 6001 △		<b>A</b>	•
NGC 4088 ▲		<b>A</b>	<b>A</b>
NGC 4172 NGC 6030			
NGC 4224			
NGC 4352 NGC 6111			

Table 1—Continued

Name	Bar	Ring	Dis	P.A.	Any	Name	Bar	Ring	Dis	P.A.	Any
NGG 1987						NGG atoa					
NGC 4375		Δ		<b>A</b>	<b>A</b>	NGC 6126					
NGC 4477	Δ			<b>A</b>	<b>A</b>	NGC 6143			<b>A</b>		<b>A</b>
NGC 4799						NGC 6155	<b>A</b>			•	<b>A</b>
NGC 4944						NGC 6196					
						NGC 6764	<b>A</b>				<b>A</b>

Table 1. Frequency of Bars, Rings and Distortions

	Sey	fert	Control			
Feature	No.	%	No.	%		
			-			
Bars	7(10)	22(31)	12(18)	24(37)		
Rings	4(8)	13(25)	4(7)	8(14)		
Dist.	8(12)	25(38)	11(13)	22(27)		
$\Theta$	10	33	11	22		
Any	21(26)	66(81)	26(31)	53(63)		